Pure Appl. Chem., Vol. 81, No. 7, pp. 1229–1239, 2009.
doi:10.1351/PAC-CON-08-10-19

Vanadium haloperoxidases as supramolecular hosts: Synthetic and computational models*

Winfried Plass

Institut für Anorganische und Analytische Chemie, Friedrich-Schiller-Universität Jena, Carl-Zeiss-Promenade 10, D-07745 Jena, Germany

Abstract: In the active-site cavity of vanadium haloperoxidases vanadate as the prosthetic group is solely fixed by one covalent bond to a histidine residue and embedded in a supramolecular environment of extensive hydrogen bonds. Structural aspects of relevant vanadium complexes with supramolecular interactions, including assemblies with chiral hosts, are presented. The importance of hydrogen-bonding relays is presented together with relevant examples. The reactivity of related functional mimics containing vanadium and molybdenum toward the oxidation of thioethers is described. Computational modeling based on density functional theory (DFT) is used for the investigation of model systems. The resulting implications for structure and function of vanadium haloperoxidases, including their substrate and cofactor specificity, are discussed.

Keywords: DFT; haloperoxidases; hydrogen bonding; supramolecular assemblies; vanadium.

INTRODUCTION

The biological and pharmacological significance of vanadium compounds has stimulated current interest in relevant vanadium chemistry. This is related to the discoveries of the insulin-like effect of vanadium compounds and the presence of vanadium in the prosthetic group of certain haloperoxidases and nitrogenases [1,2]. Key features for the understanding of how vanadium acts in biological systems are associated with the chemical analogy between vanadates and phosphates [3] on the one hand and with the supramolecular interactions through hydrogen bonding on the other hand [4].

Both features are closely related to the biological systems of vanadium-dependent haloperoxidases (V-HPOs) for which the first example was reported in 1984 by Vilter [5]. Since then, several other V-HPOs have been found in marine algae as well as in some fungi and lichens. For some of these systems, the structures have been determined by X-ray crystallography, namely, for the vanadium-dependent chloroperoxidase (V-CPO) isolated from the terrestrial fungus *Curvularia inaequalis* [6] and the bromoperoxidases (V-BPOs) isolated from the brown algae *Ascophyllum nodosum* [7] and the red algae *Corallina officinalis* [8]. The active-site structure of the V-CPOs and the V-BPOs are similar as far as the first interaction sphere is concerned. Moreover, the overall structure seems to be rather rigid as the comparison with the structures of the apoprotein and the vanadate and tungstate derivatives of V-CPO suggests [9]. The representative schematic structure of the V-CPO active site derived from *C. inaequalis* is depicted in Fig. 1.

*Paper based on a presentation at the 6th International Symposium on Chemistry and Biological Chemistry of Vanadium, 17–19 July 2008, Lisbon, Portugal. Other presentations are published in this issue, pp. 1187–1330.

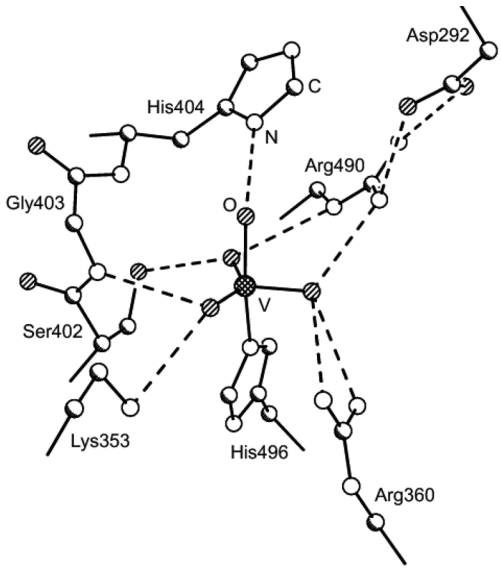

Fig. 1 Structure of the active site of V-CPO from *C. inaequalis* [6].

This group of enzymes plays an important role in synthesizing halogenated organic compounds in natural environments. V-HPOs are enzymes that catalyze the oxidation of halide ions by hydrogen peroxide to the corresponding hypohalous acids. These oxidized intermediates then readily halogenate organic substrates or convert hydrogen peroxide to singlet oxygen [10]. In addition, these enzymes are also capable of catalyzing the peroxidic oxidation of organic sulfides to sulfoxides [11]. Although a considerable number of experimental [12,13] and theoretical [14–17] studies have led to a significant advance in the understanding of the catalytic mechanism of V-HPO enzymes, there are still important issues that are unresolved. These issues are closely related to the molecular structure of the vanadate moiety in the active site, including its protonation state and the actual protonation sites [16], and how the differences in reactivity between V-CPO and V-BPO come about [18]. Of particular interest in this context is the role of the hydrogen-bonding network given by the protein matrix on structure and mode of action of the vanadate cofactor [4].

Another intriguing feature is the exceptional functional specificity of vanadate as cofactor for V-HPOs. The simplest functional model would be to employ solely the cofactor vanadate(V) [19]. On the other hand, it was found that molybdate(VI) is actually about 45 times more reactive than vanadate(V), a surprising fact that was explained by the ability of molybdate(VI) to form reactive oxo-diperoxo species [20]. Vanadate(V) is also able to form oxo-diperoxo species that nevertheless are not able to oxidize bromide ions [21]. For the enzymatic system the reconstitution of the apoprotein with molybdate(VI) instead of vanadate(V) as cofactor does not recover any catalytic activity, as was shown for the V-BPO from *A. nodosum* [5]. This is even more surprising given the fact that for structurally similar systems like the V-CPO from *C. inaequalis* and the acid phosphatase from *Escherichia blattae* the relevant tungstate(VI) [9] and molybdate(VI) assemblies [22], respectively, have been crystallographically characterized.

In contrast to the enzymatic system, functional and structural model compounds for V-HPOs generally neglect the influence of supramolecular interactions present in the protein matrix. As we believe this to be an important feature, most certainly governing structural aspects and the mode of action of V-HPOs, we recently started to address this point by utilizing synthetic and theoretical methods to study relevant model systems. In this paper, recent results along this line are summarized.

SUPRAMOLECULAR MODEL SYSTEMS

The small-molecule model chemistry of vanadium(V) complexes relevant for the haloperoxidase enzyme and its vanadate cofactor is well established [1]. We have recently started to investigate appropriate extensions toward supramolecular assemblies utilizing the versatility of the *N*-salicylidene hydrazide ligand system with the focus on the structural and functional properties of the resulting systems [4,23–26]. These tridentate chelate ligands can coordinate the vanadium moiety in either their mono- or dianionic forms. In Fig. 2, the schematic structures of relevant ligands are shown, which contain a functionalized side chain that is capable of generating supramolecular interactions with the coordinated moiety.

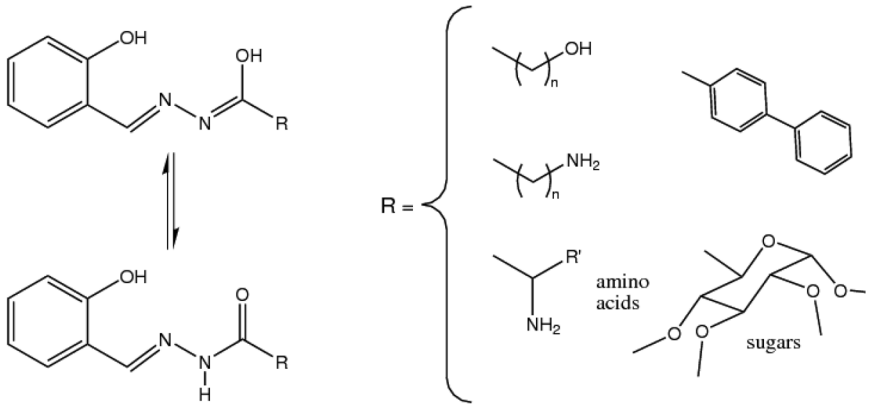

Fig. 2 Representation of *N*-salicylidene hydrazide ligands and their tautomeric forms supporting related neutral and anionic vanadium(V) complexes.

This ligand system is generally capable of supporting both oxo- and dioxovanadium(V) complexes and, moreover, also allows for the variation of the protonation state of the resulting complex leading to neutral or anionic vanadium(V) species depending on the reaction conditions [4,23].

For the ammonium salts of the dioxovanadium(V) complexes with ligands containing ω-hydroxyl side chains, interesting supramolecular structures have been obtained. In Fig. 3, the relevant structure

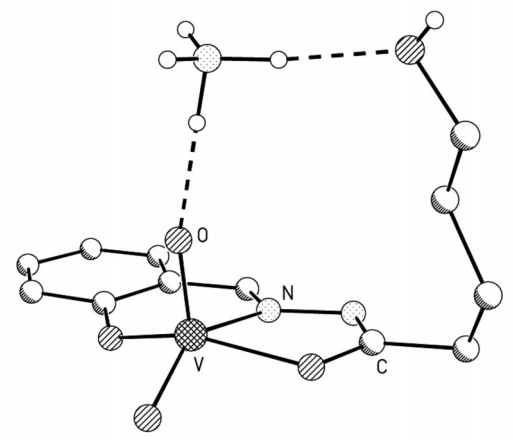

Fig. 3 Molecular structure of the ammonium salt of the dioxovanadium(V) complex with a medium length ω-hydroxyl side chain (n = 4, see Fig. 2), hydrogen bonds are drawn as broken lines [24].

for an example with medium chain length is depicted. Interestingly, variation of the side chain length does not lead to a change in the basic structure, as the ammonium cation is involved in a bridging hydrogen bond relay between the hydroxyl side chain and the vanadate moiety.

Although hydrogen bonding is a common feature for vanadium compounds in the solid state, if appropriate hydrogen-bonding donors are present [27], in the context of modeling supramolecular interactions of vanadate species relevant for biological systems, the number of known examples is rather limited [4]. Interestingly, supramolecular assemblies with hydrogen-bonding relays between the functionalized side chain and the vanadate moiety turn out to be a rather general feature for complexes with side chain functionalized *N*-salicylidene hydrazide ligand systems. In Fig. 4, two particularly interesting examples are shown. The first structure exemplifies the possible interaction with a peroxo group, resembling interactions discussed for the peroxo form of the V-CPO enzyme [28]. The second structure, derived from an amino acid derivative, is an example for protic solvent molecules, like alcohols, as hydrogen-bonded linker to oxo groups of vanadium model complexes.

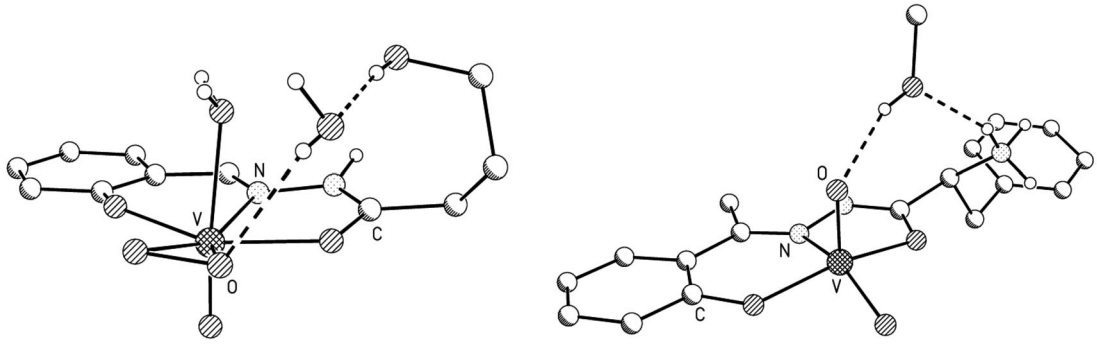

Fig. 4 Molecular structures of vanadium complexes with hydrogen-bonding relays: (left) Peroxovanadium(V) complex. (right) Phenylalanine derivative. Hydrogen bonds are drawn as broken lines [16,24].

In addition to the hydrogen-bonding relay, the phenylalanine derivative also contains a center of chirality next to the vanadium moiety. The latter feature can also be found in model complexes with ligands derived from sugars [25] and supramolecular assemblies with chiral hosts like cyclodextrins (CDs) [26]. The phenylalanine-based model complex also exhibits efficient catalytic properties with respect to haloperoxidation and sulfoxidation, which could be attributed to the influence of the free ammonium group in the vicinity of the vanadium center. It is interesting to note that even higher catalytic activity is observed for the related molybdenum(VI) complex based on a Boc-protected β-alanine derivative depicted in Fig. 5 [29]. This is an efficient catalyst for the peroxidic oxidation of sulfides, but does not show any enantioselectivity. However, if the vanadium(V) complex of a slightly modified Schiff-base ligand based on a sugar derivative is utilized, it is possible to achieve moderate enantiomeric excess depending on the substrate and the employed oxidant [30].

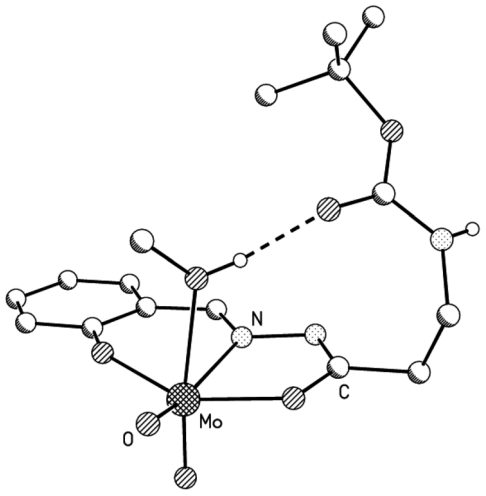

Fig. 5 Molecular structure of a molybdenum(IV) complex with a Boc-protected β-alanine derivative as ligand. Hydrogen bond is drawn as a broken line [29].

Interesting supramolecular host–guest assemblies can be obtained with CDs, if a vanadium(V) complexes with a ligand containing a biphenyl group in the side chain is employed (Fig. 6). Depending on the ring size of the CD host, different assemblies are formed. For β-CD, a 1:1 inclusion compound can be isolated [26], whereas for the smaller α-CD, two rings forming a hydrogen-bonded, head-to-head dimer host the hydrophobic biphenyl side chain of the complex [31]. It is interesting to note here that both inclusion compounds retain their structural integrity in solution as demonstrated by NMR spectroscopy.

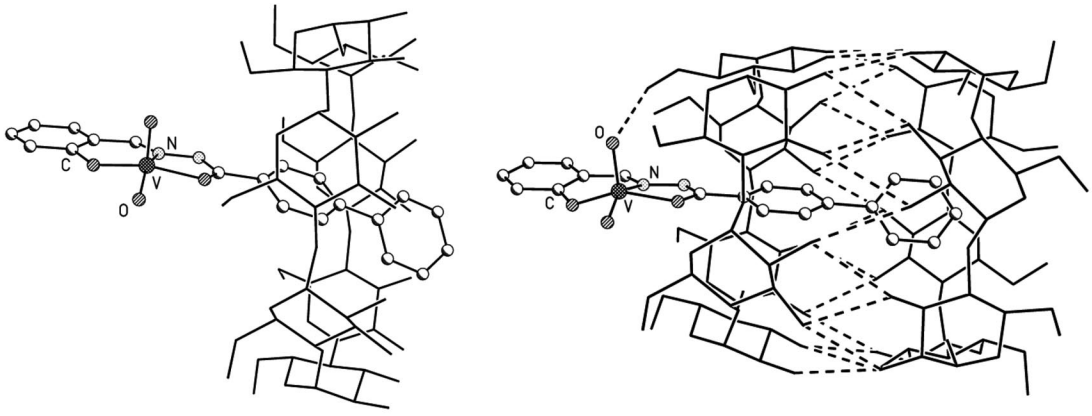

Fig. 6 Host–guest assemblies of the anionic biphenyl substituted vanadium complex $[VO_2(salhybiph)]^-$: (left) With β-CD as host. (right) With a hydrogen-bonded, head-to-head dimer of α-CDs as host. Hydrogen bonds are drawn as broken lines [26].

COMPUTATIONAL MODELS

Based on several theoretical studies, significant advances have been achieved concerning the basic understanding of the catalytic mechanism operating in small vanadate models of the V-HPO enzymes [15,32–34]. Nevertheless, the importance of the hydrogen-bonding network present in the supramolecular environment of the enzymatic systems of V-HPOs has widely been neglected when addressing relevant aspects related to their mode of action in model systems. Based on the fact that the high catalytic activity of the vanadate cofactor in these enzymes is caused by the interaction through the hydrogen-bonding network with the specifically tailored active-site pocket, the utilization of a reasonably sized approximation of the direct protein environment in terms of a model matrix is needed to address related questions. The setup of such a model matrix seems to be appropriate, as for the structure of the active-site pocket a rather high degree of rigidity is observed when various crystal structures are compared.

Utilizing the model matrix for the active-site pocket of V-HPOs depicted in Fig. 7, we have investigated the protonation behavior of the cofactor in the resting state of the enzyme [14]. Based on time-dependent density functional theory (DFT) calculations, it has been possible to identify the doubly protonated, monoanionic vanadate $[VO_2(OH)_2]^-$ (O2 and O4 protonated) as the most likely cofactor in the resting state, by comparison with the experimental UV/vis spectrum for V-CPO.

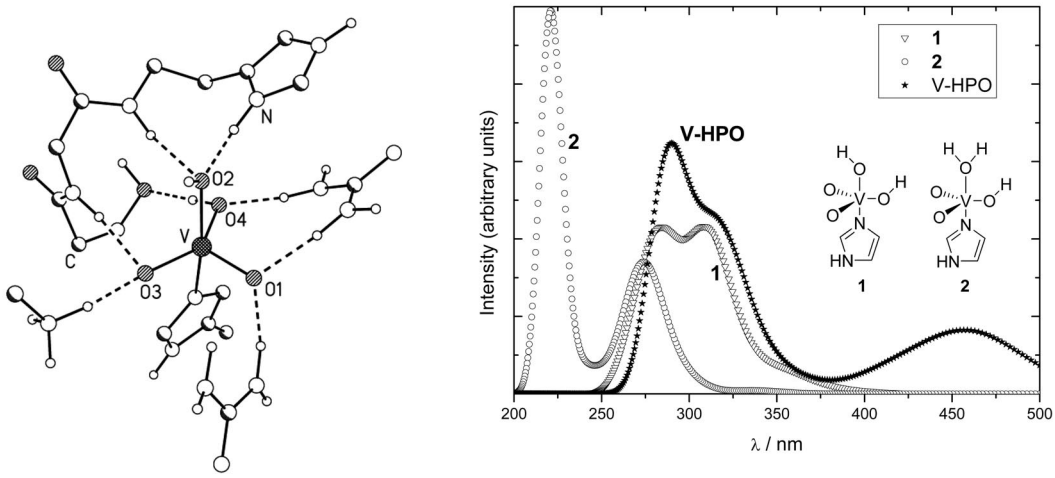

Fig. 7 V-HPO model matrix for the resting state with a $[VO_2(OH)_2]^-$ cofactor (left) and the comparison of the calculated UV/vis spectrum with those of model structures $[VO_2(OH)_2]^-$ (**1**) and $[VO_2(OH)(H_2O)]$ (**2**) [14,16].

This finding is supported by a number of theoretical studies ranging from small active-site mimics [33] to CPMD/MM (CPMD = Car–Parrinello molecular dynamics; MM = molecular mechanical) studies taking account of the protein shell [17]. Nevertheless, there is also some recent controversy, driven by QM/MM (QM = quantum mechanical) investigations, on both the actual protonation sites at the vanadate and the overall protonation state of the cofactor. In one case, a triply protonated, neutral vanadate moiety with an axially coordinated water and one hydroxyl group in the equatorial position is assumed to be the resting state [35]. Whereas another study, despite favoring a doubly protonated form of the resting state, assumes a difference in protonation sites leading to a $[VO_3(H_2O)]^-$ species with an axially coordinated water [36]. However, a recent QM/MM study comparing calculated ^{51}V NMR shift parameters with experimental data confirms the doubly protonated, monoanionic vanadate $[VO_2(OH)_2]^-$ as being the most likely candidate for the cofactor in the resting state of V-CPO [37]. Nevertheless, it is interesting to note that two additional models have been put forward in this study,

which are equally consistent with the experimental data, namely, a doubly protonated vanadate $[VO_2(OH)_2]^-$ with a shifted equatorial protonation site (cf. Fig. 7: O1 instead of O4) and a triply protonated vanadate $[VO_2(OH)(H_2O)]$ (cf. Fig. 7: O2 doubly and O3 singly protonated).

Based on the results presented recently and discussed in this contribution, including the relevant cited data from literature, the general reaction scheme depicted in Fig. 8 is proposed for the catalytic cycle of the halide oxidation by V-HPOs.

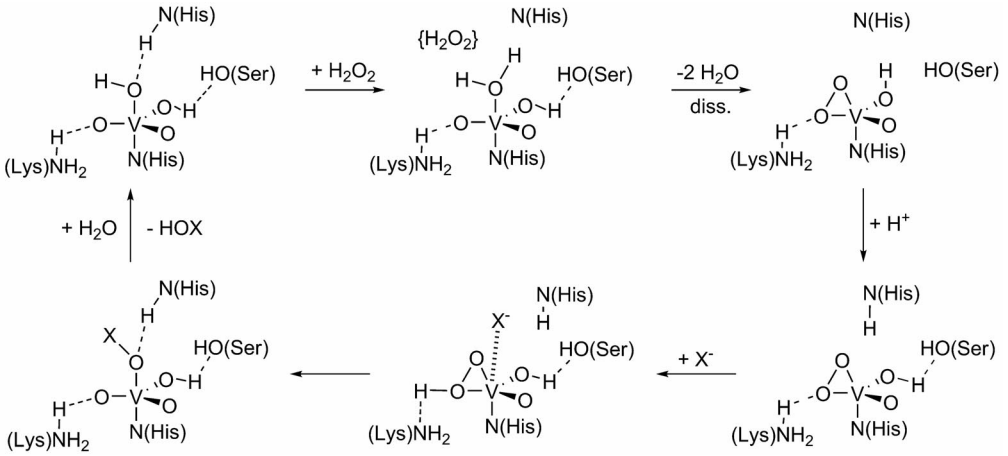

Fig. 8 Catalytic proposal for the halide oxidation by V-HPOs emphasizing the specific role of active-site residues Lys353, Ser402, and His404 (cf. Fig. 1). Charges at the vanadate are not shown.

Several aspects concerning the role of specific amino acids located in the active-site pocket (Ser402, His404, and Lys353) are worth noting here. For cases in which an equatorial hydroxyl group is present in the vanadate cofactor, the Ser402 residue most likely functions as a hydrogen-bonding acceptor for this hydroxyl group of the vanadate cofactor. This is also consistent with the fact that the Ser402 is the only acceptor within hydrogen-bonding distance for the equatorial oxygen atoms. This residue is thereby capable of defining the orientation of the $[VO_2(OH)_2]^-$ moiety in the active-site pocket. In any case, the Ser402 is certainly not involved in halide binding.

The His404 residue is proposed to be protonated in the resting state. Together with the doubly protonated vanadate this leads to a situation that represents a latent apical water molecule. It should be possible to bring this masked water molecule to action by subtle changes in the electronic structure of the vanadate cofactor, which might be triggered by an initial stimuli like the incoming substrate hydrogen peroxide (or even the halide ion), since strong hydrogen-bonding donors stabilize the resting-state situation of a latent water molecule, i.e., the proton located at the His404. In fact, this might also explain why the newly reported triple mutant P395D/L241V/T343A of the V-CPO of *C. inaequalis* is operating at a considerable higher pH optimum [13], as the hereby introduced aspartate residue Asp395 can be expected to reduce the hydrogen-bonding ability of possible donors (e.g., Arg360) toward equatorial oxygen atoms.

Unlike the situation observed for model complexes, where a protonation is required to initiate the formation of the peroxo species, the enzyme affinity toward hydrogen peroxide is even increasing at higher pH values. This is consistent with the proposed high degree of protonation for the resting state of the enzyme, thereby offering all essential prerequisites for the transformation without any additional proton source. Moreover, based on the pK_a values of hypohalous acids and histidine, it can be assumed that the enzyme thus does not need to take any particular precaution to facilitate the availability of protons. Therefore, formally a proton and a halide ion X^- are added in a successive manner during the

cycle. Nevertheless, a general feature needed, not only in the formation of the peroxo form of the enzyme, but also in the control of the halide oxidation step, are proton-transfer reactions, which might be facilitated by proton transmitters or acid–base catalysts as is exemplified by the proton relays observed for the model complexes.

Besides the basic considerations concerning the mode of action of the V-HPO system, there are two additional intriguing features of this system, namely, the specificity toward the processed halide ion as V-CPO and V-BPO are compared and the strict cofactor preference for vanadate, despite the superior reactivity of molybdate.

The halide specificity has been argued to possibly originate from differences in the outer sphere of the active-site structure evident from the crystallographic data obtained for V-CPO from *C. inaequalis* [6] and V-BPO from *A. nodosum* [7]. It was proposed that the His411 residue present in the structure of V-BPO, which aligns with Phe397 in V-CPO, should be responsible for the observed differences in reactivity. In Fig. 9, the structural difference with respect to the vanadate cofactor and the lysine residue in the active-site pocket (Lys353 in V-CPO and Lys341 in V-BPO) is depicted. It was originally suggested by Weyand et al. that this can be attributed to an additional direct proton donor/acceptor interaction with the peroxo form of the cofactor [7], where the latter is found to be oriented toward the Lys353 [28].

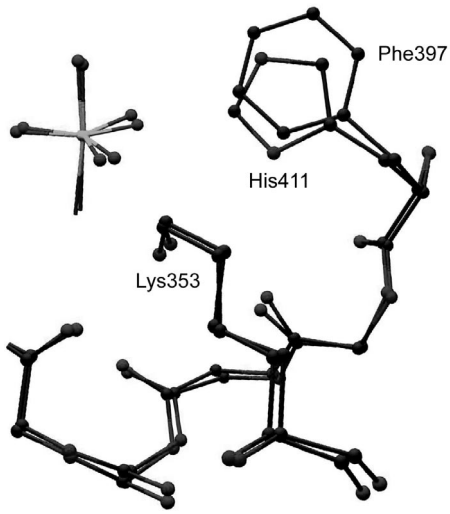

Fig. 9 Overlay of the active-site structure of V-CPO from *C. inaequalis* [6] and V-BPO from *A. nodosum* [7]. The Lys353 residue in the vicinity of the vanadate cofactor is denoted according to the V-CPO notation, whereas the difference in the second sphere given by the His411 in place of a Phe397 residue is denoted according to the original V-BPO and V-CPO notation, respectively.

On the basis of DFT investigations on a small peroxovanadate mimic for the reaction with halide ions, Zampella et al. have argued that reducing the polarizing ability of the employed RNH group, modeling the role of Lys353, by additional anionic counterions strongly diminishes the ability of the cofactor toward halide oxidation. Consequently, they proposed that the possible additional hydrogen bond from the lysine to the histidine could buffer the polarizing power of the Lys353 [34].

In fact, detailed DFT investigations for an extended model system, with hydrogen-bonding relay from histidine over lysine toward the peroxo form of the vanadate cofactor, including charge flow analysis clearly show that the electrophilicity of the not involved oxygen atom of the peroxo group can be triggered by the underlying relay. This is particularly obvious as the variation in charges and relevant parameters of bond critical points for corresponding transition states are compared. The results suggest

that subtle differences in the arrangement of the hydrogen-bonding pattern allow for the tuning of the degree of activation of the peroxo group within the active-site pocket of V-HPOs.

In order to understand why the enzymatic system prefers vanadate(V) instead of choosing the catalytically more active molybdate(VI) as cofactor, DFT calculations on model systems mimicking the initial steps in formation of the peroxo form have been performed. Based on recent results, the most likely mechanism follows a dissociative reaction path starting from a triply protonated vanadate [$VO_2(OH)(H_2O)$] (cf. Fig. 7: O2 doubly and O3 singly protonated) [16]. The structures of the initial steps along this path are depicted in Fig. 10.

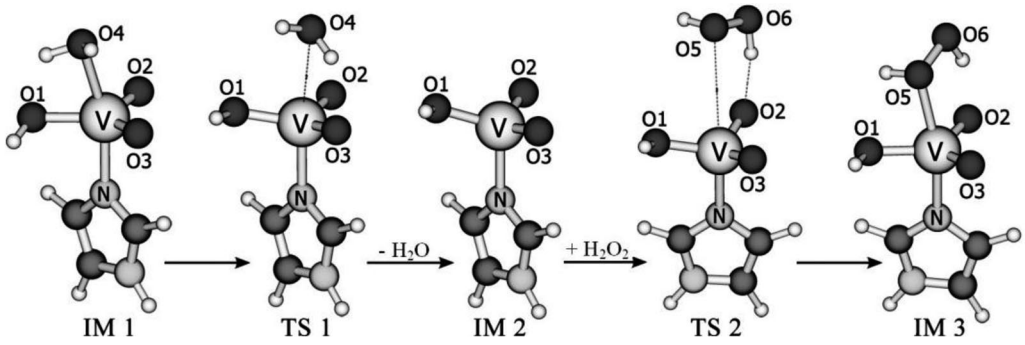

Fig. 10 Intermediate (IM) and transition state (TS) structures for the initial steps of the formation of the reaction of hydrogen peroxide with imidazole-bound vanadate.

The results obtained show that the oxo-diperoxo species [$MoO(O_2)_2Im$] is indeed more catalytically active than the dioxo-monoperoxo species [$MoO_2(O_2)Im$] consistent with experimental evidence [20]. However, the spatial environment of the VHPO active site is tailored to a monoperoxo species. Calculations investigating the halide oxidation activity of the molybdenum(VI) monoperoxo species allow the conclusion that [$MoO_2(O_2)Im$] exhibits some catalytic activity—apparently a contradiction to earlier results reported by Vilter obtained from studies on the V-BPO system [5]. Presumably, the actual reason for the inactivity of "molybdenum bromoperoxidase" might be that no peroxo species is formed in the first place.

Ongoing studies hence explore the formation of the molybdenum monoperoxo species [38]. The first and central step of the dissociative mechanism is the cleavage of water (Fig. 10) and the subsequent attack by hydrogen peroxide. Since molybdenum generally supports larger coordination numbers as compared to vanadium, it can be assumed that it prefers an associative reaction mechanism rather than the dissociative favored for vanadium. In order to verify this claim, structures of several stationary points on the potential surface along the reaction coordinate for this first dissociative step of the catalytic cycle were calculated for both the vanadium and the molybdenum species (Fig. 10). Activation energy barriers and Gibbs free reaction energy values for both species were calculated from the free energy values of the optimized structures. This indeed leads to significant difference, as the reaction of hydrogen peroxide with [$VO_2(OH)(H_2O)Im$] is an *exergonic* process ($\Delta_R G = -18.6$ kJ/mol), while the same reaction employing [$MoO_2(OH)(H_2O)Im$] is *endergonic* ($\Delta_R G = +24.0$ kJ/mol). Consequently, together with the steric tuning of the active-site pocket, this may prevent the formation of a relevant peroxo species embedded in the V-HPO apoenzyme and thereby account for the missing haloperoxidase activity.

CONCLUSIONS

For the structure and reactivity of the vanadate cofactor in V-HPOs, the supramolecular environment given by the protein matrix is a key feature. A series of vanadium complexes capable of modeling the supramolecular interactions found for vanadate in biological systems has been presented. This includes well-established host–guest systems of appropriate complexes with CDs for which both the solution and the solid-state structures have been determined. A particular feature of model complexes containing side chain functionalized *N*-salicylidene hydrazide ligand systems is the generation of hydrogen-bonding relays including the vanadate moieties. This is a feature also relevant for functional aspects of the V-HPO enzymes. Vanadium and molybdenum complexes with related ligands are found to be functional mimics, which in particular are capable of catalytically oxidizing thioethers. Based on our theoretical results, a picture of the mode of action of the V-HPO systems is presented, that includes interpretation of some specific roles of amino acid residues of the active site interacting with the vanadate cofactor. The specific reactivity of V-CPO and V-BPO with respect to the oxidation of the halide ion substrate can be explained in terms of a hydrogen-bonding relay. This relay extends from a histidine residue (His411 in V-BPO) in the second coordination sphere of the cofactor via the catalytically important lysine residue (Lys341 in V-BPO; Lys353 in V-CPO), which in turn is in hydrogen-bonding contact with the vanadate cofactor. Moreover, computational modeling based on DFT has been used to demonstrate the differences in reactivity of vanadate and molybdate cofactor with respect to the V-HPO enzymatic environment. Finally, the presented examples clearly show that V-HPO enzymes are supramolecular hosts with important prerequisites to appropriately fine-tune the relevant mode of action by hydrogen-bonding relays.

ACKNOWLEDGMENTS

The Deutsche Forschungsgemeinschaft for their generous support by a research grant as well as the John von Neumann Institute for Computing (NIC–JUMP supercomputer) at the Forschungszentrum Jülich and the computer center of the Friedrich-Schiller-University for supplying computational time are gratefully acknowledged. The results presented in this review are based on the engagement and outstanding skills of many coworkers who are named in the literature citations.

REFERENCES

1. D. C. Crans, J. J. Smee, E. Gaidamauskas, L. Yang. *Chem. Rev.* **104**, 849 (2004).
2. (a) H. Sigel, A. E. Sigel (Eds.). *Vanadium and its Role in Life*, Vol. 31 of *Metal Ions in Biological Systems*, Marcel Dekker, New York (1995); (b) K. H. Thompson, J. H. McNeill, C. Orvig. *Chem. Rev.* **99**, 2561 (1999); (c) K. Kustin, J. Costa Pessoa, D. C. Crans (Eds.). *Vanadium: The Versatile Metal*, ACS Symposium Series No. 974, American Chemical Society, Washington, DC (2007).
3. W. Plass. *Angew. Chem., Int. Ed.* **38**, 909 (1999).
4. W. Plass. *Coord. Chem. Rev.* **237**, 205 (2003).
5. H. Vilter. *Phytochemistry* **23**, 1387 (1984).
6. A. Messerschmidt, R. Wever. *Proc. Natl. Acad. Sci. USA* **93**, 392 (1996).
7. M. Weyand, H. J. Hecht, M. Kiess, M. F. Liaud, H. Vilter, D. Schomburg. *J. Mol. Biol.* **293**, 595 (1999).
8. M. N. Isupov, A. R. Dalby, A. A. Brindley, Y. Izumi, T. Tanabe, G. N. Murshudov, J. A. Littlechild. *J. Mol. Biol.* **299**, 1035 (2000).
9. A. Messerschmidt, R. Wever. *Inorg. Chim. Acta* **273**, 160 (1998).
10. (a) G. W. Gribble. *Acc. Chem. Res.* **31**, 141 (1998); (b) R. Wever, W. Hemrika. In *Handbook of Metalloproteins*, Vol. 2, A. Messerschmidt, R. Huber, T. Poulos, K. Wieghardt (Eds.), pp. 1417–1428, John Wiley, Chichester (2001).

11. (a) M. Andersson, A. Willetts, S. Allenmark. *J. Org. Chem.* **62**, 8455 (1997); (b) H. B. ten Brink, H. E. Schoemaker, R. Wever. *Eur. J. Biochem.* **268**, 132 (2001).
12. (a) R. Renirie, W. Hemrika, S. R. Piersma, R. Wever. *Biochemistry* **39**, 1133 (2000); (b) C. Kimblin, X. H. Bu, A. Butler. *Inorg. Chem.* **41**, 161 (2002); (c) N. Tanaka, Z. Hasan, R. Wever. *Inorg. Chim. Acta* **356**, 288 (2003).
13. Z. Hasan, R. Renirie, R. Kerkman, H. J. Ruijssenaars, A. F. Hartog, R. Wever. *J. Biol. Chem.* **281**, 9738 (2006).
14. M. Bangesh, W. Plass. *J. Mol. Struct. Theochem.* **725**, 163 (2005).
15. (a) J. Y. Kravitz, V. L. Pecoraro. *Pure Appl. Chem.* **77**, 1595 (2005); (b) C. Schneider, G. Zampella, L. De Gioa, V. L. Pecoraro. In *Vanadium: The Versatile Metal*, ACS Symposium Series No. 974, K. Kustin, J. Costa Pessoa, D. C. Crans (Eds.), p. 148, American Chemical Society, Washington, DC (2007).
16. W. Plass, M. Bangesh, S. Nica, A. Buchholz. In *Vanadium: The Versatile Metal*, ACS Symposium Series No. 974, K. Kustin, J. Costa Pessoa, D. C. Crans (Eds.), p. 163, American Chemical Society, Washington, DC (2007).
17. S. Raugei, P. Carloni. *J. Phys. Chem. B* **110**, 3747 (2006).
18. J. Littlechild, E. Garcia-Rodriguez, E. Coupe, A. Watts, M. Isupov. In *Vanadium: The Versatile Metal*, ACS Symposium Series No. 974, K. Kustin, J. Costa Pessoa, D. C. Crans (Eds.), p. 136, American Chemical Society, Washington, DC (2007).
19. M. J. Clague, A. Butler. *J. Am. Chem. Soc.* **117**, 3415 (1995).
20. (a) V. Conte, F. Di Furia, S. Moro. *J. Phys. Org. Chem.* **9**, 329 (1996); (b) G. E. Meister, A. Butler. *Inorg. Chem.* **33**, 3269 (1994); (c) A. F. Ghiron, R. C. Thompson. *Inorg. Chem.* **29**, 4457 (1990).
21. A. Butler, A. H. Baldwin. *Struct. Bonding* **89**, 109 (1997).
22. K. Ishikawa, Y. Mihara, K. Gondoh, E. Suzuki, Y. Asano. *EMBO J.* **19**, 2412 (2000).
23. (a) W. Plass, A. Pohlmann, H.-P. Yozgatli. *J. Inorg. Biochem.* **80**, 181 (2000); (b) W. Plass, H. P. Yozgatli. *Z. Anorg. Allg. Chem.* **629**, 65 (2003).
24. (a) A. Pohlmann, W. Plass. *J. Inorg. Biochem.* **86**, 381 (2001); (b) S. Nica, A. Pohlmann, W. Plass. *Eur. J. Inorg. Chem.* 2032 (2005); (c) A. Pohlmann, S. Nica, T. K. K. Luong, W. Plass. *Inorg. Chem. Commun.* **8**, 289 (2005); (d) S. Nica, M. Rudolph, H. Görls, W. Plass. *Inorg. Chim. Acta* **360**, 1743 (2007); (e) S. Nica, A. Buchholz, M. Rudolph, A. Schweitzer, M. Wächtler, H. Breitzke, G. Buntkowsky, W. Plass. *Eur. J. Inorg. Chem.* 2350 (2008).
25. J. Becher, I. Seidel, W. Plass, D. Klemm. *Tetrahedron* **62**, 5675 (2006).
26. I. Lippold, H. Görls, W. Plass. *Eur. J. Inorg. Chem.* 1487 (2007).
27. (a) W. Plass. *Z. Anorg. Allg. Chem.* **623**, 461 (1997); (b) W. Plass. *Eur. J. Inorg. Chem.* 799 (1998).
28. A. Messerschmidt, L. Prade, R. Wever. *Biol. Chem.* **378**, 309 (1997).
29. M. Mancka, W. Plass. *Inorg. Chem. Commun.* **10**, 677 (2007).
30. I. Lippold, J. Becher, D. Klemm, W. Plass. *J. Mol. Catal. A: Chem.* **299**, 12 (2008).
31. I. Lippold, K. Vlay, H. Görls, W. Plass. *J. Inorg. Biochem.* **103**, 480 (2009).
32. (a) V. Conte, O. Bortolini, S. Carraro, S. Moro. *J. Inorg. Biochem.* **80**, 41 (2000); (b) O. Bortolini, M. Carraro, V. Conte, S. Moro. *Eur. J. Biochem.* 42 (2003).
33. G. Zampella, J. Y. Kravitz, C. E. Webster, P. Fantucci, M. B. Hall, H. A. Carlson, V. L. Pecoraro, L. De Gioia. *Inorg. Chem.* **43**, 4127 (2004).
34. G. Zampella, P. Fantucci, V. L. Pecoraro, L. De Gioia. *J. Am. Chem. Soc.* **127**, 953 (2005).
35. J. Y. Kravitz, V. L. Pecoraro, H. A. Carlson. *J. Chem. Theory Comput.* **1**, 1265 (2005).
36. Y. Zhang, J. A. Gascón. *J. Inorg. Biochem.* **102**, 1684 (2008).
37. M. P. Waller, M. Bühl, K. R. Geethalakshmi, D. Wang, W. Thiel. *Chem.—Eur. J.* **13**, 4723 (2007).
38. D. Geibig, R. Wilcken, M. Bangesh, W. Plass. *NIC Series* **39**, 71 (2008).